NASA CR 71094

GPO PRICE $ _____

CFSTI PRICE(S) $ _____

Hard copy (HC) 2.00

Microfiche (MF) .50

ff 653 July 65

WYLE LABORATORIES
TESTING DIVISION, HUNTSVILLE FACILITY

WYLE LABORATORIES - RESEARCH STAFF
Report WR 65-26

PREDICTION OF THE INFLIGHT FLUCTUATING PRESSURES ON SPACE VEHICLES

By

M.V. Lowson

Work performed under Contract NAS8-11308

Prepared by M.V. Lowson
M.V. Lowson

Approved by Kenneth McK. Eldred
Kenneth McK. Eldred
Director of Research

December 1965

COPY NO. 42

SUMMARY

19532

This report presents a review of current data on the pressure fluctuations encountered by space vehicles during their ascent through the lower atmosphere. Complete data on these fluctuating pressure sources is not yet available, and much of the available data is fragmentary and inconsistent. However, the need for the prediction of these fluctuating pressures is very distinct and this report gives methods for this prediction based on currently available results.

The sources considered include attached boundary layer turbulence, separated flow turbulence, oscillating shock waves, protuberance flows, jet impingement, cavity response phenomena, and base pressure fluctuations. Emphasis has been placed on separated flow and oscillating shock phenomena. Typical levels for each source are given as a function of vehicle Mach number, geometry, and total head. Frequency spectra and correlation areas are also given where possible.

Author

TABLE OF CONTENTS

LIST OF TABLES

LIST OF FIGURES

1.0 INTRODUCTION

The major sources of vibration on a space vehicle during boosted flight are due to the aerodynamically induced fluctuating pressures that act upon the vehicle skin. These sources include

Attached Boundary Layer Turbulence
Separated Flow Turbulence
Oscillating Shock Waves
Protuberance Flows
Jet Impingement
Cavity Response Phenomena
Base Pressure Fluctuations

A number of methods for predicting the characteristics of these fluctuating pressure sources have previously been published, notably that by Eldred, Roberts, and White (Reference 1.1)*. The present report is an extension of this work to include the more recent information that has become available. However, even now, both experimental and theoretical information on many of the fluctuating pressure sources is fragmentary. For this reason it is not possible to make any precise statements of the anticipated fluctuating loadings, and the predictions made here are the result of an empirical correlation of the available data reinforced, where possible, by arguments from first principles. Only broad statements of the fluctuating mechanisms and limitations of the predictions will be given. More detailed discussions may be found in the quoted references (see Section 9.0).

For each source the designer requires information about four basic parameters: position and extent, magnitude, frequency spectrum, and correlation pattern. Each source represents a separate prediction problem, and will be dealt with in turn below. The case of the attached turbulent boundary layer will be discussed first, not because of its significance, but because it is the one fluctuating pressure phenomenon which can be described with some precision. It therefore forms a good basis for the discussion of the less well understood sources of fluctuation.

The initial task, however, is to determine the probable sources of fluctuation on each part of the vehicle. Section 2.1 gives a general discussion of the source characteristics to assist solution of this problem, and Section 2.2 gives a general discussion of the problems of predicting frequency spectra. The following sections give detailed methods for calculating the fluctuating pressure characteristics of various sources. Readers who require only an order of magnitude figure for the levels of fluctuating pressure are referred to Figure 1 and Table I.

*References are given in a decimal numbering system and are listed in Section 9.0

2.0 GENERAL DISCUSSION

2.1 The Problem of Predicting Overall Levels

The first problem in prediction is to define the probable sources of excitation at all vehicle stations. Fortunately, the position and extent of each type of source is related to the steady state flow patterns that occur on the vehicle, and the steady flow is governed primarily by vehicle geometry and Mach number. (Mach number is the vehicle velocity divided by the velocity of sound in the free stream).

A completely smooth aerodynamically "clean" body would maintain an attached turbulent boundary layer over almost the whole surface. For such a case prediction is relatively straightforward because of the rather extensive experimental data that have now been gathered on the problem (see Section 3.0). Unfortunately the majority of present and future generation space vehicles are the antithesis of the classical low drag aerodynamic design and it is unlikely that a fully developed attached turbulent boundary layer exists anywhere on the surface of a modern vehicle (see Figure 1). The most significant sources of fluctuating pressure on the majority of space vehicles will be in the region of separated flow and oscillating shocks. Such regions will be found at transonic speeds immediately behind the cone-cylinder shoulders of multistage vehicles, and at supersonic speeds in the cylinder-cone compression corner areas. Further details of the position and extent of the pressure fluctuations due to separated flow and oscillating shocks may be found in Section 4.0.

In principle, the flow over the remaining part of the vehicle corresponds to an attached boundary layer case, but in practice there are innumerable projections on the surface of a modern space vehicle, each producing a turbulent wake. Perhaps the most important of these on manned space vehicles is the wake from the escape tower which passes over the whole vehicle and has been observed to increase fluctuation levels by well over 10 dB compared to the "clean" case (Ref. 1.5 and 2.4)., however, each projection will produce local increases in level, and at supersonic speeds the shock patterns associated with each projection will stream over the vehicle. For an overall study the only practical possibility is to make some general empirical allowance to include all these effects. However, designers should be cautioned to study the structural characteristics near each projection to ensure that the locally increased levels of fluctuation cannot be potentially damaging. The effects of protuberances are discussed in Section 5.0.

Two major sources of fluctuating loading can be the impingement of jet or rocket exhausts, (Section 6.0) and cavity responses (Section 7.0). However, the possibility of these phenomena occurring can usually be eliminated in the design stages. The predicted levels of fluctuation will normally be sufficient to require that the exhausts be pointed away from the structure and that any cavities be covered. One further source of unsteady loading is that of the base pressure fluctuations (Section 8.0) caused by the swirling turbulent flow at the base of the vehicle. The levels of this phenomenon are relatively low, particularly when compared to the near-noise field of the rocket exhaust which the base structure must endure on take off. It should be noted that the sound field of the rocket exhaust can cause significant loadings,(Reference 1.1), especially on the rear

part of the vehicle. These direct acoustic loadings are normally limited to the first few seconds of take off, but will also occur during static test firing of the vehicle.

The magnitude of sources of fluctuating pressure has generally been found to be substantially proportional to the dynamic head q ($= 0.5 \rho U^2$, where ρ is the density and U the free stream velocity) with only secondary effects of Mach number and Reynolds number. For this reason the first step in any prediction sequence is to determine the total head of the rocket as a function of time and Mach number. For cases when the trajectory is not available, reference may be made to Figure 2 which gives typical values for a large launch vehicle. The sections which follow will give the magnitude of the pressure fluctuations in the non-dimensional form of p_{rms}/q (root mean square pressure fluctuation divided by total head). The actual levels of pressure fluctuation can therefore be obtained from this form by multiplication by the appropriate total head. For convenience, Figure 3 gives a direct conversion from p_{rms}/q to sound pressure level in dB* for various values of q.

Many of the prediction methods discussed below require a knowledge of the approximate boundary layer thickness at various points on the body. Accordingly, Figure 4 gives the boundary layer thickness calculated from $\delta = 0.37 \times Re^{-0.2}$ (Reference 3.18). This formula only applies strictly to the case of an incompressible boundary layer on a smooth flat plate so that some error must be expected in application to a three-dimensional supersonic case. A further error in Figure 4 arises from the assumption that viscosity has its ground level value. However, in view of the other uncertainties in the problem these errors are unlikely to be significant.

In this report the values given are those which are thought to be the most likely. In cases like the present where so little real knowledge exists it is tempting to give conservative estimates at all stages of the prediction, and thus finally arrive at answers which may be orders of magnitude too high. Here, the most probable values are given throughout, but in view of the uncertainty it will usually be desirable to add some safety factor to the final figure depending on the use to which the prediction will be put. An additional factor of 5 dB would be typical.

It should be pointed out that all discussion in this report refers to the conditions on an unyawed vehicle with the free stream directed along the axis. Probably only minor, and predictable, changes will occur up to angles of attack of 3°, but for angles of attack above 5° there is a possibility of cross flow separation. This results in a pair of vortices appearing over the vehicle which may have high local fluctuating pressures beneath them. Unfortunately, very little is known about the effect, at least from the fluctuating pressure standpoint, although values of $p_{rms}/q \approx 0.1$ have been reported for the equivalent case on a delta wing (Reference 3.9). Present flight results indicate that the fluctuating pressure levels can be increased on the leeward side of the vehicle by about 1 dB per degree of angle of attack.

*In this report all decibel (dB) levels are referred to 0.00002 Newton/m^2(0.0002 dyne/cm^2)

2.2 Problems in Predicting Frequency Spectra

Prediction of the frequency spectrum of the fluctuating pressures from first principles is extremely difficult. At the present time, the subsonic attached turbulent boundary layer is the only source phenomenon which has been studied in detail, and this is only of limited relevance to a practical problem. In principle the spectrum of any given source should scale on a Strouhal number basis providing the source mechanisms are similar. Strouhal number is a non-dimensional measure of the frequency formed by multiplying the frequency (f) by a typical length (ℓ) divided by a typical velocity (U). Thus the conversion from model parameters (suffix m) to vehicle parameters (suffix v) is given by

$$S = \frac{f_m \ell_m}{U_m} = \frac{f_v \ell_v}{U_v}$$

The critical problem comes in the choice of suitable "typical" lengths and velocities. In nearly all fluctuating pressure phenomena 'Taylors hypothesis' is found to apply, that is; the observed fluctuating pressures are the result of the convection of an almost stationary pressure pattern past the observation point. In principle therefore, all that is required is a definition of the typical scale of such a pressure pattern and its convection velocity. Clearly, the division of the typical velocity by the typical length should give the typical frequency. In practice, such velocities and lengths cannot be specified even for the thoroughly studied case of the attached turbulent boundary layer. It seems that each frequency component is associated with different "typical" velocities and lengths, and that the complete fluctuation phenomenon cannot be defined in simple terms. For more complex fluctuating pressure sources the possibilities of defining such velocities and lengths are correspondingly reduced.

Direct conversion to full scale from results from a model of identical configuration may be accomplished using any relevant dimension and velocity, providing other scale effects, such as those due to Reynolds' number, can be ignored. Strouhal scaling using diameter and free stream velocity has usually been successful in predicting full scale frequency spectra from model tests. However, scaling of the results between different configurations requires a knowledge of the source mechanisms which does not, at present, exist.

For example, the spectra of the fluctuating pressures on full scale Saturn I vehicle were predicted with good accuracy by Strouhal scaling of the experimental results obtained on models of the vehicle. A comparison is shown in Figure 5 taken from Ref. 2.9. It may be observed that the peak third octave band frequency was about 50 cps. Full scale frequency spectra for the 21 foot diameter Saturn I vehicle typically lie within a range of 50-200 cps, over a range of flow types, stations,and Mach numbers. In contrast, results from recent tests on a ten inch diameter research model at Ames (Reference 4.14) would suggest full scale frequencies below 10 cps beneath a supersonic oscillating shock,

while results from the Scout vehicle (Reference 2.3) would suggest Saturn scale peak frequencies around 500 cps. It is clear that no consistent prediction of frequency spectrum of the fluctuating aerodynamic pressures can be made on the basis of present knowledge.

Fortunately, the application of Strouhal scaling is usually satisfactory for identical configurations. Figure 5 shows the type of agreement that can occur, although it should be noted that this is an exceptionally favorable example. However, reasonable agreement is usually obtained. Thus full scale predictions can be made when model test data exist for the particular vehicle under consideration. However, such data will not always be available, and Figure 6 has been prepared to offer some broad guidance in such cases. This figure shows typical octave band spectrum shapes from a variety of vehicles. These spectra cover a very wide variety of flow conditions, Mach number, and vehicle station, and have been referred to overall level and also non-dimensionalized on the basis of vehicle diameter and velocity. In view of the wide variation in parameters the spectra could hardly be expected to show close agreement, but some general similarities can be observed. Note that the ranges shown in Figure 6 for each set of results include only those specific results which seem typical, and are not envelopes of all results observed. Surprisingly, no consistent effect of vehicle station has been observed. It is presumed that the anticipated increase in scale towards the rear of the vehicle is balanced by large scale tower wake effects at the front of the vehicle, although this cannot be the whole answer.

Figure 6 also shows a suggested prediction curve. It should be made clear that this curve is an extremely crude empirical approximation, to be used only in the absence of any more relevant data. However, in such cases it may be helpful in defining some of the broad features of the inflight fluctuating pressure spectra. The prediction curve corresponds to the formula

$$\overline{p^2(f)} = \frac{2 f_0}{\pi (f_0^2 + f^2)}$$

where $\overline{p^2(f)}$ is the mean square sound pressure per cps, f is frequency, and f_0 is a typical (peak octave band) frequency. In Figure 6 $f_0 D/V$ has been put equal to 2. There is some evidence (notably in References 2.3 and 2.6) that values of $f_0 D/V$ are higher for supersonic flow than for subsonic flow, and this is in accord with results from the acoustic generation by rocket exhaust flows. This observation could be taken into account by putting $f_0 D/V = 1$ for subsonic flows and $= 4$ for supersonic flows. However, not all data show this trend and at the present time no definite statements can be made on the significance of the effect.

The prediction curve of Figure 6 gives asymptotic octave band levels falling away at 3 dB per octave at both the high and the low ends of the spectrum. This corresponds to a white noise spectrum at low frequencies and a 6 dB per octave fall off in mean square pressure/cps at high frequencies. At both high and low frequencies this is expected to be conservative, but has been retained because of the relatively small proportion of energy contained at either of these predicted extremes.

In the sections which follow more detailed predictions of frequency spectrum will be given where possible. The empirical curve discussed above applies to the type of pressure fluctuation phenomena currently encountered on space vehicles and will be referred to again during the discussions.

3.0 THE ATTACHED TURBULENT BOUNDARY LAYER

On a large space vehicle, the flight Reynolds number ($U\ell/\nu$, where U is velocity, ℓ is length from front of vehicle, and ν is kinematic viscosity) will reach approximately 10^9 shortly before max q. Experimentally, it is found that the boundary layer will usually undergo a transition from a smooth 'laminar' to an irregular 'turbulent' flow at Reynolds numbers near 5×10^5. Even in the very favorable circumstances of supersonic flow over a nose cone the boundary layer will undergo transition to turbulence below Reynolds numbers of 10^7. Thus, the full scale vehicle will always be under the action of the pressure fluctuations caused by turbulent boundary layer flows at least until it reaches altitudes greater than about 40 km (130,000 ft) when it will generally be travelling at hypersonic ($M > 5$) speeds.

An undisturbed flat plate turbulent boundary layer flow is unlikely to occur anywhere on the vehicle because of the unusual vehicle geometry coupled with the profusion of projections. Nevertheless, the results obtained during the last few years on this classical problem are of great assistance in the interpretation and prediction of more complex effects.

It is found that the turbulent boundary layer produces surface pressure patterns which are convected along the skin at velocities varying between 0.5 and 0.8 of the free stream velocity. These patterns have been linked to the convected eddy structure of the turbulent boundary layer. A considerable amount of information is now available on the fluctuation levels, frequency spectra, and correlation patterns of the pressure fluctuations produced by subsonic turbulent boundary layers. There are little data for the supersonic case, but the rather limited work of Kistler and Chen (Reference 3.14) indicated that the supersonic case was not too seriously different from the subsonic case, and this finding enabled the subsonic results to be applied to the supersonic case with some hope of success.

Eldred, Roberts, and White, in Reference 1.1, gave a reduction of all the available boundary layer data, and showed how both subsonic and supersonic data reduced to give a uniform level of $p_{rms}/q = 0.0052$. The supersonic data in this case were obtained during aircraft flight and had a tendency to be somewhat lower than this figure. Much of the currently available data from supersonic wind tunnels tends to be slightly higher than this value, possibly due to the effects of tunnel noise and turbulence. However, it should be pointed out that a large proportion of the subsonic data has been filtered in a rather arbitrary way to remove part of the low frequency noise. Serafini, in Reference 3.10, made careful experimental wind tunnel measurements which retained most of the low frequencies and found $p_{rms}/q \approx 0.0075$. On the other hand, Hodgson has made measurements on a glider (reported in Reference 3.4), which show a very small low frequency content, and give values of $p_{rms}/q < 0.005$.

Thus the balance of the experimental evidence is that a value of $p_{rms}/q \approx 0.005$ gives a fairly good prediction of the pressure fluctuations in an attached turbulent boundary

layer on a body in free flight, at both subsonic and supersonic speeds. This value is probably somewhat conservative for supersonic flight, while for subsonic flight $p_{rms}/q \approx 0.006$ would be more typical. However, nearly all model wind tunnel tests will have higher levels of fluctuation, mostly in the lower frequencies so that the overall levels would be raised by about 50 percent.

For the subsonic attached boundary layer it is possible to define typical frequency spectra and correlation patterns. The low frequency content of the fluctuation can still not be defined with any confidence, as mentioned above. However, the moderate and high frequency content is found to scale on a Strouhal number basis. There has been much discussion in the literature about the correct typical lengths and velocities to choose for this Strouhal non-dimensionalization, and there is inevitably one choice of length and velocity which gives the best reduction for any given set of data. However, application of the various suggested non-dimensionalizing parameters to other sets of results is not encouraging. Thus, in this report, the suggested non-dimensionalizing parameters are the total boundary layer thickness δ and the free stream velocity U. These parameters have the advantage of being used elsewhere in the report and also of being readily calculable. In view of the other uncertainties this method should not lead to any significant additional error.

The suggested frequency spectrum for the attached turbulent boundary layer is shown in Figure 7. For the moderate and high frequencies this represents the mean of results from Bull, (Reference 3.1), Serafini (Reference 3.10), and Willmarth (References 3.12 and 3.13), corrected for finite transducer size. However, the low frequency part of the curve is pure speculation. Theoretical estimates due to Lilley, (Reference 3.3), supported by Hodgson's experimental work on a glider, (Reference 3.4), suggest a lower level at the low frequencies, but Serafini's work indicates a much higher level. The low frequency part of the predicted curve in Figure 7 is based on the belief that Serafini's results were primarily a tunnel effect. Note that the overall level of the empirical curve in Figure 7 corresponds to $p_{rms}/q = 0.006$, the typical level at subsonic speeds.

Information on the correlation lengths of the eddies is somewhat inconsistent. Lighthill (Reference 1.6), found the pressure pattern to have a correlation radius of $1.2\,\delta$ and to be moving at a velocity of $0.82\,U_0$. It is known that the velocity fluctuations in the boundary layer are more correlated in the free stream direction than in the lateral direction, but Bull, (Reference 3.1), found the correlation lengths to be $0.4\,\delta$ longitudinally and $0.84\,\delta$ laterally. In fact, correlation area and convection velocity will vary with the frequency component under consideration, and the whole problem is highly complex. For engineering purposes it is suggested that the pressure patterns be assumed to have a correlation radius equal to the boundary layer thickness (δ) and to be moving at $0.8U_0$. In some cases it will be desirable to estimate correlation length as a function of frequency. It is suggested that the correlation radius be taken as half the wavelength for high frequencies, and as the boundary layer thickness for frequencies with wavelengths more than twice the boundary layer thickness. This suggestion is supported by a number of physical arguments, and is in broad agreement with tht experimental results on coherence length reported by Bull in Reference 3.1.

4.0 SEPARATED FLOW AND OSCILLATING SHOCKS

Separated flow and oscillating shocks, often in combination, provide the most significant acoustic environment encountered by a space vehicle during its ascent through the atmosphere. Boundary layer separation will occur when a boundary layer meets a sufficiently adverse (rising) pressure gradient. On a space vehicle such conditions are encountered behind the interstage shoulders at subsonic and transonic ($0.8 < M < 1.2$) speeds, and in the interstage compression corners at supersonic ($M > 1.2$) speeds (see Figure 1). These two types of flow have different characteristics, and will be treated in separate sections.

4.1 The Supersonic Case

At supersonic speeds a turbulent separated flow and associated oscillating shock usually form in front of the cylinder-cone interstage junctions. The complete flow field is highly complex, and no satisfactory theoretical solution of this case exists, even for the mean flow. Empirical analysis of the existing experimental data has given some information, (Reference 4.16), but it is clear that a complete empirical description of the flow including the full effects of body geometry and Mach number would be far more complicated than could be justified by the present uncertainties in knowledge. Thus, in this report, the supersonic separated flow will be discussed using an approximation suggested in Reference 4.16. This is, that the separated flow forms a fillet in the compression corner which has a constant angle of 12.5°, unaffected by body geometry or Mach number, (see Figure 8a).

This approximation is only strictly true for Mach numbers near 2.0, and for a limited range of body geometries. However, it is acceptable for practical applications to the present case. For the majority of presently conceived vehicles the flow will reattach to the surface at the top shoulder of the interstage region. Given this, the assumption of a 12.5° separation zone defines the extent of the separation and the position of the separation point. The principal limitation on this assumption is the possible effects of step height for very pronounced differences in stage diameter. The separation region would then be smaller than predicted above. It will also be observed that with the present method no separation is predicted for flare angles of less than 12.5°. This is an acceptable approximation from the fluctuating pressure viewpoint, although limited regions of separation could be encountered for flare angles down to 10°. Further details of the limitations of the approximation may be found in Reference 4.16.

The general character of the fluctuating pressures in the interstage compression corner due to separated flow at supersonic speeds is shown in Figure 8b. The fluctuating pressures reach a peak level at the front of the separated region. This first peak level is associated with the existence of an oscillating "separation" shock located above the surface at that point. The fluctuation level then reduces to a rather low value for a substantial length of the separation region but rises towards the reattachment point to a level roughly equal to that of the initial peak. The details of this second peak level are probably dependent

on the geometry of the body in the reattachment zone. The results obtained by Kistler, (Reference 4.15), differ substantially from those obtained by Coe, (Reference 4.14). The suggested levels for the peak fluctuating pressure coefficient (p_{rms}/q) at both the forward and aft peaks are given as a function of Mach number in Figure 9. This figure is based on results from Reference 4.14, and represents an envelope of the higher levels obtained. However, this should not be construed as a conservative estimate since Kistler's results (Reference 4.15), although somewhat limited in range, indicated still higher peak values with p_{rms}/q reaching 0.1. The lower level of fluctuation reached within the separated flow is not a strong function of Mach number and seems to be approximately constant at $p_{rms}/q = 0.025$. The exact variation of level within the separation region cannot be specified with any accuracy. A typical form is shown in Figure 8b, although Kistler, (Reference 4.15), found an approximately linear rise from immediately behind the first peak to the second peak at the rear of the separation. It is suggested that the given variation in level be simplified as required for each prediction.

The position of the first peak may sometimes be critical in terms of panel excitation. It should be born in mind that the present method for prediction of position via the 12.5° angle is only an engineering approximation. This angle will probably always lie within the limits of 9° to 17°, and the designer should take into account a possible variation within these limits when investigating the possible local significance of this peak loading for any particular panel. The width of the first peak is another unknown factor. The data of Reference 4.14 suggests that it be taken as about half the local boundary layer thickness. Boundary layer thickness may be estimated using Figure 4; see also Section 3.0.

A separated flow can cause significant pressure fluctuations even at remote stations downstream. This is because the large scale turbulent eddies associated with the separation do not undergo recirculation within the separated region, but proceed downstream past the point of reattachment. An example of this is the turbulent wake from the escape tower which causes high levels of fluctuations over a substantial portion of the forward part of the vehicle. Figure 10 shows some typical levels for this fluctuation occurring in flight at supersonic speeds, although the effect of Mach number has been found to be relatively small, so that those levels may be applied at other speeds. It will be observed that the direct effect of the wake is little higher than that of the attached boundary layer after two diameters. However, it should be noted that this wake could still have significant effect on the fluctuations occurring beneath oscillating shocks via shock-turbulence interaction. Although no data on this point is currently available it is anticipated that other separated flows will have similar, although smaller, effects downstream of their reattachment point. A rough estimate could be found using Figure 10 and halving both the level and extent.

Prediction of the frequency spectrum for the pressure fluctuations due to the separated flow and oscillating shock is yet another extremely difficult problem. Experimental evidence is not yet in agreement as to the random or discrete nature of the frequency pattern. In view of this discrepancy it would hardly be realistic to expect any possibility for a

detailed spectrum prediction. However, the experimental evidence points to the probability that these fluctuations are quick to couple with any available source of excitation. In a model test this could be wind tunnel noise or model resonances, while in the full scale case such sources could arise from vehicle oscillations, local panel flutter,or atmospheric disturbances. Perhaps the most likely source of excitation is the vehicle turbulent boundary layer and this is also suggested (inconclusively) by model tests. Theoretical study suggests that shock turbulence interaction could be a leading cause of surface pressure fluctuation (Reference 4.16). Recent model tests, (Reference 4.14), have shown a rather low peak frequency beneath the oscillating shock, with a higher peak (octave band) frequency beneath the separated flow. However, there is, as yet, insufficient evidence to draw any firm conclusions on this effect.

Coe pointed out in Reference 4.13 that the overall amount of energy appeared to be constant and adopted a frequency distribution to suit the excitation, but it would clearly be over-pessimistic to assume that the source spectrum exactly matched the response spectrum. For an engineering estimate it is suggested that all possible excitation sources,- panel resonances, vehicle motion, atmospheric fluctuations , and vehicle boundary layer - be considered to derive a probable excitation spectrum, and that a mean be derived between this spectrum and the typical source spectrum presented in Figure 6. This procedure should produce a predicted spectrum which reflects a moderate allowance for the effects of the response on the source characteristics. If desired, it is suggested that the correlation radius be taken as equal to the equivalent attached boundary layer thickness as in Section 3.0.

4.2 The Subsonic and Transonic Case

Experiment reveals the subsonic and transonic flow fields around a multi-stage launch vehicle to be highly complex and configuration dependent. The flows are also found to be markedly dependent on Reynolds number, so that there is little experimental information which can be reliably applied to any new configuration at full scale Reynolds numbers.

In general, the largest levels of fluctuating pressure will occur beneath the oscillating shocks which terminate the supersonic region immediately behind the vehicle shoulders. However, the extent of this fluctuation is relatively small, as is the duration of the fluctuation at any particular station. The fluctuating pressures caused by the turbulent wake from the escape tower are also found to be of major significance, particularly over the forward portions of the vehicle surface. Unfortunately there is little experimental data on the effect of the escape tower at transonic speeds beyond that of Jones and Foughner, (Reference 2.4). In addition, tower configurations may change radically from vehicle to vehicle, so that the present predictions of acoustic environment could well be significantly altered by a change in tower design, see also Sections 4.1 and 5.0.

A sufficiently supersonic flow will almost always be attached to the surface behind the shoulder. However, in the subsonic-transonic regime there seem to be five different types of flow which can occur behind a cone-cylinder shoulder:

1) Wholly subsonic attached flow.

2) Wholly subsonic separated flow.

3) Attached supersonic flow terminated by a shock followed by attached subsonic flow.

4) Attached supersonic flow terminated by shock followed by locally separated subsonic flow.

5) An alternating condition in which the flow alternates between a subsonic separated and one of the supersonic attached cases.

The boundaries between these flows cannot be defined with any precision. For cone angles less than 10° the flow will usually be type 1 up to about $M = 0.9$ when it will change to type 3. For cone angles above 30° the flow will normally be type 2 until very close to $M = 1$ when it will change to type 3. But the majority of actual vehicle configurations lie between these two extremes and it is very difficult to make any definite statement about the type of flow that will occur. The problem is further complicated by the marked effect which the presence of the escape tower has on the flow characteristics. The predictions which follow should therefore be regarded as gross simplifications which could easily be in error.

In all cases supersonic flow immediately behind each shoulder will occur at a sufficiently high Mach number, and it has been found that the shockwave terminating the supersonic region moves back downstream as the Mach number increases. A correlation of the available experimental results on shock position as a function of Mach number is shown in Figure 11, taken from Reference 4.16. These results are derived, in the main, from the first shoulder of a simple cone cylinder model, so that there could be some doubt as to their applicability to subsequent shoulders, or to cases with escape towers (see below). High levels of fluctuating pressure are found immediately under the shock, presumably due to local shock oscillations. These levels are shown as a function of Mach number in Figure 12, taken from Reference 4.16. It will be observed that no consistent configuration effects can be observed in either of Figures 11 and 12. However, the points on Figure 11 do correlate reasonably well and the curve shown has been drawn through them. The results shown in Figure 12 do not show a very clear trend. The curve drawn for Figure 12 is based on semi-empirical reasoning (Reference 4.16), and is suggested as a prediction curve.

The highest level reached by the fluctuating pressures beneath the shock appears to be a function of cone angle and Figure 12 gives suggested limits for the 15° and 20° cone cases. Experimental information on shock position and fluctuating pressures at shoulders subsequent to the first is very sparse. Some results for the second shoulder which do correlate with those for the first are shown in Figure 12. But it should be noted that other tests have found results which are not in good agreement. In general, the shock seems to be further forward than anticipated. There is some evidence that the same effect may occur in the presence of the escape tower. It can only be suggested that the results of Figures 11 and 12 are applied to all vehicle shoulders until more experimental information is available.

The extent of the fluctuating pressures beneath the oscillating shock is about 0.2 diameters. Outside this region lower values for the fluctuation level apply. For the tower off case the levels are very much lower and it is suggested that p_{rms}/q be taken as about 0.01, although there is some possibility that a separated flow will exist behind the shock (flow type 4 above). Current experimental information indicates that this type flow is confined to a narrow range of cone angles near 20°. In such a case fluctuation levels might reach $p_{rms}/q \approx 0.025$. Rather large magnitudes of fluctuating pressure have been recorded beneath the wholly subsonic separated flow (type 1 above). There is considerable scatter in the data but a typical value is $p_{rms}/q \approx 0.1$, (also suggested in Reference 1.1). In the lack of more definitive information this flow may be assumed to occur for cone angles greater than 22°. The extent of this subsonic separation is also a matter of some conjecture. Available results indicate a reduction to a level of $p_{rms}/q \approx 0.01$ over about two diameters behind the shoulder.

The alternating flow separation and attachment (type 5 above, see Reference 4.8), is not a significant practical source of fluctuating pressures. During model tests levels of $p_{rms}/q \approx 0.2$ have been recorded, but the condition is highly sensitive to Mach number, and in flight the vehicle would accelerate through the critical Mach number range in less than 0.3 second , which is less than the expected alternation period for the phenomenon. No alternating condition would therefore be anticipated. However, the sudden change from subsonic separated to supersonic attached flow could provide a significant shock loading to the vehicle, which may require consideration during design.

Some results for the effect of the tower wake have already been given in Figure 10. Jones and Foughner, (Reference 2.4), give results for the pressure fluctuations at the first shoulder which show broadly comparable results for the tower wake at transonic speeds. Their results also showed how by the second shoulder the tower was causing fluctuations of $p_{rms}/q \approx 0.015$. This level existed for about a diameter behind the shoulder and was the result of interaction between the wake and the supersonic flow behind the shoulder. It is suggested that the results of Figure 9 be used for prediction of the transonic effects of the tower on the first shoulder, and that an allowance of $p_{rms}/q \approx 0.01$ be added for one diameter behind any subsequent shoulders.

It will be observed that there are two rather different sources of excitation at transonic speeds. The first is due to the oscillating shocks and separated flow caused by the basic vehicle geometry and the second is due to the wake shed by the escape tower. When two such independent sources are in action, experiment indicates that for levels of $p_{rms}/q > 0.025$ approximately the larger source dominates at any station, whereas for lower levels of excitation the sources are additive. Thus, the peak levels occurring immediately behind the shoulders due to oscillating shocks are substantially unaffected by the tower wake while the lower levels occurring in the flow downstream of the oscillating shocks are increased when the tower is present.

The comments on the prediction of frequency spectrum for the supersonic separated flows and oscillating shocks (Section 4.1), apply equally to the transonic case. Again it is suggested that the source spectrum be taken as the mean of the anticipated excitation and the empirical curve of Figure 6, and that correlation radius be taken as equal to boundary layer thickness.

5.0 PROTUBERANCE FLOWS

The comparative unimportance of "clean" aerodynamic design on space vehicles has led to the addition of great numbers of protuberances of all kinds on external surfaces. Indeed, predictions of pressure fluctuations based on unadorned vehicle geometry may be considerably in error if the various flows from protuberances are not considered. Each protuberance has two effects, the direct action near to the protuberance itself and the downstream wake.

Prediction of the average geometry and fluctuating characteristic of each wake would be possible within the present state of the art. However, there are so many protrusions of all types on a modern space vehicle that the calculations would hardly be justified. On the basis of currently available data it is recommended that an allowance of $p_{rms}/q = 0.01$ be added to the predicted levels to account for the various wakes which may be present. For the near wake behind the protuberance the fluctuations may be assumed to decay to that level over about 10 protrusion dimensions from a higher level of about $p_{rms}/q = 0.05$. However, each protuberance may cause significant levels of pressure fluctuation in its immediate vicinity through the action of separated flows and oscillating shocks. The protuberance can generate transonic buffet loadings over its upper surfaces and cause upstream separated flow regions to form at supersonic speeds. The unusual geometry of many protuberances will often cause the pressure fluctuations generated in these regions to be relatively high. A figure of $p_{rms}/q \approx 0.1$ is suggested for the fluctuation under the supersonic oscillating shock to account for the increased shock strength due to three-dimensionality.

The critical parameter governing the severity of the fluctuating pressures is the ratio of the protuberance height to the boundary layer thickness. Clearly, protuberances lying well within the boundary layer would not be expected to be important sources of pressure fluctuation, whereas those which extended well outside the boundary layer would generate their own external flow field. It is very unlikely that any model test could duplicate the relative scale of boundary layer and protuberance that will occur in flight so that, in general, it will not be possible to acquire valid experimental results. This is particularly true of the transonic tests, and for this case no accurate estimate of the position or extent of the buffet loading is possible, although it is perhaps possible to set an upper limit for the magnitude using the data of Section 4.2.

The only case where prediction may be possible is for a large and relatively clean protrusion. Even here the difficulties of predicting the enveloping three dimensional flow field are formidable. For some supersonic cases it may be possible to use the data of Section 4.1 to make a broad prediction. But very little is known of the properties of a three dimensional separated flow. Some basic information on the mean flow was given in Reference 5.1, where the flow around a cylinder protruding from a surface was studied. It was found that the surface boundary layer separated in front of the freestream shock surrounding the cylinder, so that a second separation shock surface acted as a

partial fillet between the cylinder shock and the surface. For low enough cylinder heights the cylinder shock was not apparent. The complexities of this relatively simple case illustrate the difficulties of dealing with protuberance flows.

In general, it has been found that the protuberances add energy in the low frequencies, (References 3.13 and 5.2). However, no precise prediction of the exact spectrum is justified at present, and it is suggested that the empirical curve of Figure 6 be used for the frequency spectrum. This spectrum has been derived from results on practical "dirty" vehicles and is expected to be reasonably representative. However, for the regions of oscillating shocks it is suggested that the panel response and other such excitation phenomena be taken into account as suggested in Section 4.1. Again, a correlation radius equal to boundary layer thickness is suggested.

6.0 JET IMPINGEMENT

A space vehicle has numbers of venting jets, ullage and retro rockets, and other exhaust flows which can impinge on the structure. Such impingement will give rise to high levels of fluctuating pressure. Fortunately, other considerations will normally require that the exhausts be pointed away from the surrounding structure. Further, it is expected that the magnitude of the fluctuating loadings, together with the associated high-temperatures will generally be sufficient to persuade the designer to avoid any flow impingement, although this may not always be possible at high altitudes where the jet flow expands through a fairly large angle.

Again very little data is available. Lilley and Hodgson, (Reference 3.4), studied the pressure fluctuations in the flow formed several diameters away from a jet impinging normally on the wall. Their results suggest that the fluctuating pressure intensity immediately under the jet could reach $p_{rms} = 0.1\, q_j$; where q_j is the total head of the jet ($= 0.5\, \rho\, U_j^2$). This figure is suggested for design purposes for both normal and oblique jet impingement. Based on Lilley and Hodgson's results it is anticipated that the fluctuating pressures would reduce at about 12 dB per doubling of radius from the jet.

It would be possible to give detailed methods for predicting frequency spectra based on arguments from measured velocity spectra in free jets, as in Reference 1.1. However, this complication is not thought to be justified, and here it is suggested that the empirical curve of Figure 6 be used with jet diameter and velocity as the non-dimensionalizing parameters. The results of Lilley and Hodgson are in broad agreement with this approach except that the present method produces an over conservative estimate for the low frequencies. This difference is not significant. Correlation radius could be taken equal to jet radius for engineering estimates.

7.0 CAVITY RESPONSE PHENOMENA

The problem of cavity responses may often be solved in the design stages by eliminating the cavities themselves, but when the presence of cavities becomes unavoidable then the acoustic resonances will represent a serious source of loading. It has been found that the cavity response phenomena may be split into two types, one is the discrete frequency resonance response, primarily associated with short or deep cavities, and the other type of response is a random buffet response which assumes equal importance for long or shallow cavities. The fluctuating pressure amplitude of the resonant cavity response can reach $p_{rms}/q = 0.35$, (Reference 7.5).

It appears that the mechanism causing the cavity resonance is the vortex-sound wave feed back loop familiar in studies of edge tones, noise of over pressure supersonic jets, etc., (References 7.1, 7.3, and 7.5), and the whole phenomenon is governed by the acoustic response of the cavity. Rossiter, (Reference 7.5), gives a series of shadowgraphs demonstrating the downstream propagation of the vortices and the upstream propagation of the acoustic pulse, which appears as a shock wave in his photographs.

However, the most important practical feature of cavity resonance phenomena has still to be mentioned: the discrete frequency resonant response may be eliminated by making the front end of the cavity an irregular shape. Simple experiments at Wyle Laboratories have indicated that the cavity resonance disappears with the addition to the front edge of a projection about a tenth of cavity width and about half local boundary layer thickness. Rossiter's work, (Reference 7.5), indicated successful resonance suppression with a spoiler spanning one eighth of the cavity width and about 0.75 of the local boundary layer thickness in height. The projection should be located roughly in the center of the cavity for highest effectiveness. Rossiter's results indicate that the typical pressure fluctuation with the spoiler in place is random in nature with $p_{rms}/q \approx 0.02$.

Short or deep cavities will usually exhibit resonance to various degrees. The maximum $p_{rms}/q = 0.35$ was recorded on an 8 inch long by 8 inch deep by 2 inch wide cavity at $M = 0.9$. It is suggested that such cavities be covered, or at least provided with a suitable spoiler. However, long or shallow cavities will generally not have significant resonance response, presumably because of the effect of the geometry on the vortex in the feed back loop. Unfortunately, another effect comes into prominence for shallow cavities. The rear face acts like a forward facing step and produces high buffet loadings ($p_{rms}/q \approx 0.1$) due to the action of separated flows and oscillating shocks. These loadings are also found to act on the skin immediately behind the cavity. The methods of Sections 4.1 and 4.2 will give a general idea of the magnitudes to be expected here.

Length, width, and depth of the cavity all affect the response phenomena, but sufficient information is not at present available to give a systematic discussion of their effects. If the presence of a cavity on the vehicle is unavoidable the designer is referred to References 7.3 and 7.5 which present complete discussions of the response phenomena. In applying

the results of Plumblee, Gibson, and Lassiter, (Reference 7.3), some care is recommended. Their boundary layer noise measurements are some 20 dB below results obtained by other workers and there is some indication that their other results may be similarly in error. This does not affect the validity of their work on response mechanisms and resonant frequencies.

8.0 BASE PRESSURE FLUCTUATIONS

Immediately behind the rocket there is a large scale turbulent recirculating region which can cause fluctuating pressures on the base of the vehicle. At the present time virtually no experimental information exists on these fluctuating pressures at supersonic speeds. However, some subsonic results have been reported by Eldred, (Reference 8.1), and these must necessarily form the basis for any prediction technique. Eldred found that the base levels of fluctuation at the center of a circular base region were relatively low but doubled at the 65 percent radius position , (Figure 13). This effect is presumed to be the result of the relatively stagnant flow that must exist towards the center of the base.

Eldred's results show good internal consistency and it is tempting to extend these results to the supersonic case. Figure 13 also shows some data obtained by Coe, (Reference 4.14), on the pressure fluctuations occurring immediately behind a step at supersonic speeds. These figures are assumed to correspond to the levels appearing at the center of a base flow. In that case the level at 65 percent radius might be assumed to be double that of these experimental points. It will be observed that the levels of p_{rms}/q show a pronounced reduction with increase in Mach number. There is some independent evidence in support of this phenomena in that the static pressure levels in the base pressure region show a similar tendency. Since no reliable information is yet available on base pressure fluctuations at supersonic speeds the empirical curve shown in Figure 13 is suggested for prediction.

Prediction of the frequency spectrum of the fluctuations may be accomplished via Eldred's experimental results. He found that the spectra collapsed well using a Strouhal number based on base diameter. Since the base flows may be expected to be subsonic at even high supersonic speeds there would be little reason to expect a major change in this finding. Eldred's experimental spectrum shape is shown in Figure 14.

On a real vehicle the base will not be a simple plane surface, but will mount several rockets, each generating a high velocity exhaust. In fact, it is not thought that these exhausts will have too important an effect on the low speed recirculating flow. During lift-off the noise generated by the rocket exhausts can penetrate the base region and cause very high levels of acoustic excitation (perhaps 165 dB), but it is not anticipated that the presence of the exhaust flow will have too important an effect in flight. It is found experimentally that some exhaust gas does flow into the base region, and this can cause high temperatures up to about Mach 3, but after this point the overall base flow is out of the base region as it adjusts to the reduced ambient pressure at high altitudes. One (unpublished) measurement of base pressure fluctuations has been made in flight, and this showed a substantially constant level at about 152 dB for all Mach numbers up to 3 (apart from the lift off phase). However, there is some question as to the vibration effects on these measurements, and this figure may perhaps be regarded as an upper bound.

9.0 BIBLIOGRAPHY AND REFERENCES

This bibliography is not exhaustive but is intended to provide a sample of the more relevant information on each of the fluctuating pressure phenomena. For convenience the reports are grouped under headings which broadly correspond to the organization of the present report, and cross references are given where necessary.

1. General Summary Reports

1.1 Eldred, K., Roberts W., and White R., "Structural Vibrations in Space Vehicles", WADD Tech. Rep. 61-62, Dec. 1961.

1.2 Franken P.A., and Kerwin E.M., "Methods of Flight Vehicle Noise Prediction", WADC TR 58-343

1.3 Franken P.A., "Methods of Space Vehicle Noise Prediction", WADC TR 58-343, Vol. II.

1.4 Lowson M.V., "The Aerodynamically Induced Pressure Fluctuations on Space Vehicles", Wyle Laboratories Report WR 64-5, October 1964.

1.5 Rainey A.G., "Progress on the Launch Vehicle Buffetting Problem", J. Spacecraft and Rockets, Vol 2, No. 3, May-June 1965.

1.6 Lighthill M.J., "Sound Generated Aerodynamically", Proc Roy Soc (London) A Vol 267, pp 147-182, 1962.

2. General Experimental Data

2.1 Ailman C.M., "Wind Tunnel Investigation of the Fluctuating Pressures on the Surface of a Saturn I Vehicle 2.75 Percent Model", NASA CR 53435, Douglas SM-44148A, August 1963.

2.2 Garcia S., "Aerodynamic Analysis of Saturn I Block I Flight Test Vehicles", NASA TN D-2002, February 1964.

2.3 Garrick I.E., Hilton D.A., and Hubbard H.H., "Recent Free-Flight Boundary-Surface Aerodynamic Noise Measurements", AGARD Report 467, 1963.

2.4 Jones G.W., and Foughner J.T., "Investigation of Buffet Pressures on Models of Large Manned Launch Vehicle Configurations", NASA Technical Note D-1633, May 1963.

2.5 Mayes W.H., Hilton D.A., and Hardesty C.A., "In Flight Noise Measurements for Three Project Mercury Vehicles", NASA TN D 997, Jan. 1962.

2.6 North American Aviation Inc., "Transient Pressure Measurements Apollo Wind Tunnel Model PSTL-2".

2.7 Shiffer R.A., "Correlation of Launch-Vehicle Wind-Tunnel Aerodynamic Noise with Spacecraft Flight Vibration Data", JPL T R 32-619, May 1964.

2.8 Young G., and Shiokari T., "Buffeting Data Obtained on Mercury/Atlas MA2 and MA3", TDR-594(1101) TN-1 Aug. 1961.

2.9 George B.W., "Acoustic Environment Study for the Saturn IB Launch Vehicle", Lockheed MSC TM 54/20-20, Jan 1965.

3. Attached Boundary Layer Turbulence

3.1 Bull M.K., "Properties of the Fluctuating Wall-Pressure Field of a Turbulent Boundary Layer", AGARD Report 455, 1963.

3.2 Harrison M., "Pressure Fluctuations on the Wall Adjacent to a Turbulent Boundary Layer", 2nd Symposium on Naval Hydrodynamics pp 107-126, Aug 1958.

3.3 Lilley G.M., "Pressure Fluctuations in an Incompressible Turbulent Boundary Layer", CoA Rep 133, June 1960.

3.4 Lilley G.M., and Hodgson T.H., "On Surface Pressure Fluctuations in Turbulent Boundary Layers", AGARD Report 276, 1960.

3.5 Lowson M.V., "Pressure Fluctuations in Turbulent Boundary Layers", NASA TN D3156, December, 1965

3.6 Mull H.R., and Algranti J.S., "Preliminary Flight Survey of Aerodynamic Noise on an Airplane Wing", NACA RM E55K07, March 1956.

3.7 Mull H.R., and Algranti J.S., "Flight Measurement of Wall-Pressure Fluctuations and Boundary-Layer Turbulence", NASA TN D-280, October 1960.

3.8 Murphy J.S., Bies D.A., Speaker W.V., and Franken P.A., "Wind Tunnel Investigation of Turbulent Boundary Layer Noise as Related to Design Criteria for High Performance Vehicles", NASA TN D-2247 April 1964.

3.9 Richards E.J., and Doak P.E., "Some Practical Applications of Boundary Layer Pressure Fluctuation Work", AGARD Report 468 1963.

3.10 Serafini J.S., "Wall-Pressure Fluctuations and Pressure-Velocity Correlations in a Turbulent Boundary Layer", NASA TR R-165, April 1964.

3.11 Willmarth W.W., "Space-Time Correlations and Spectra of Wall Pressure in a Turbulent Boundary Layer", NASA MEMO 3-17-59W, March 1959.

3.12 Willmarth W.W., and Wooldridge C.E., "Measurements of the Fluctuating Pressure at the Wall Beneath a Thick Turbulent Boundary Layer, Journal of Fluid Mechanics, Vol 14, Part 2, October 1962.

3.13 Willmarth W.W., "Corrigendeun: Measurements of the Fluctuating Pressure at the Wall Beneath a Thick Turbulent Boundary Layer", J.F.M. 21 prl pp 107-109, Jan 1965.

3.14 Kistler A.L., and Chen W.S., "A Fluctuating Pressure Field in a Supersonic Turbulent Boundary Layer", J. Fluid Mech. Vol 16, pp 41-64, May 1963.

3.15 Lilley G.M., "Wall Pressure Fluctuations Under Turbulent Boundary Layers at Subsonic and Supersonic Speeds", AGARD Report 454, 1963.

3.16 McLeod G., "Flight Determined Aerodynamic Noise Environment of an Airplane Nose Cone up to a Mach No. of 2", NASA TN D1160.

3.17 Williams D.J.M., "Measurements of the Surface Pressure Fluctuations in a Turbulent Boundary Layer in Air at Supersonic Speeds", Dept. of Aeronautics and Astronautics, Southampton University, Report 162.

3.18 Schlicting H., "Boundary Layer Theory", McGraw Hill 4th Ed., 1960

See also 1.1.

4. Separated Flows and Oscillating Shocks

4.1 Bogdonoff S.M., "Some Experimental Studies of the Separation of Supersonic Turbulent Boundary Layers", Proc. Heat Transfer Fluid Mech Inst, 1955.

4.2 Chapman D.R., Kuehn D.M., and Larson H.K., "Investigation of Separated Flows in Supersonic and Subsonic Streams With Emphasis on the Effects of Transition", NACA Rep 1356.

4.3 Cooke, J.C., "Separated Supersonic Flow", Technical Note No. Aero 2879, Royal Aircraft Establishment, March 1963.

4.4 Kuehn D.M., "Boundary-Layer Separation Induced by Flares on Cylinders at Zero Angle of Attack", NASA TR R-117, 1961.

4.5 Sanders F., and Crabtree L.F., "A Preliminary Study of Large Regions of Separated Flow in a Compression Corner", RAE-TN 2751, March 1961.

4.6 Trilling L., "Oscillating Shock Wave Boundary Layer Interaction", J.A. Sc., pp 301-311, May 1958.

4.7 Vasiliu J., "Pressure Distribution in Regions of Step-Induced Turbulent Separation", J.A. Sc. V 29 No. 5, pp 596-601 and 631, May 1962.

4.8 Chevalier H.L., and Robertson J.E., "Pressure Fluctuations Resulting From an Alternating Flow Separation and Attachment at Transonic Speeds", AEDC-TDR-63-204.

4.9 Coe C.F., "Steady and Fluctuating Pressures at Transonic Speeds on Two Space-Vehicle Payload Shapes", NASA TM X-503, March 1961.

4.10 Coe C.F., "The Effects of Some Variations in Launch-Vehicle Nose Shape on Steady and Fluctuating Pressures at Transonic Speeds", NASA TM X-646, March 1962.

4.11 Coe C.F., and Kaskey A.J., "The Effects of Nose Bluntness on the Pressure Fluctuations Measured on 15° and 20° Cone-Cylinders at Transonic Speeds", NASA TM X-779, January 1963.

4.12 Coe C.F., and Nute J.B., "Steady and Fluctuating Pressures at Transonic Speeds on Hammerhead Launch Vehicles", NASA TM X-778, December 1962.

4.13 Coe C.F., "The Effect of Model Scale on Rigid Body Unsteady Pressures Associated With Buffeting", Proc. Symp. Aero Elastic Dynamic Modeling Tech. Dayton Ohio, 23-25 Sept. 1963. RTD-TDR-63-4197 Pt II.

4.14 Coe C.F., Unpublished Experimental Work at NASA Ames Research Center.

4.15 Kistler A.L., "Fluctuating Wall Pressure Under a Separated Supersonic Flow", JASA Vol. 36 No. 3, pp 543-550, March 1964.

4.16 Lowson M.V., "The Acoustic Environment Due to Separated Flow and Oscillating Shocks", Wyle Laboratories Quarterly Progress Report for April, May and June 1965 on Contract NAS8-11308.

See also References in Section 2.0, particularly 2.4.

5. Protuberance Flows

5.1 Halprin R.W., "Step Induced Boundary Layer Separation", AIAA Journal Vol 3 No. 2, p 357, Feb 1965.

5.2 Jorgensen D.W., "Measurements of Fluctuating Pressures on a Wall Adjacent to a Turbulent Boundary Layer", D.T.M.B. Underwater Acoustics Office R. and D. , Rep 1744, 1963.

See also 3.13.

6. Jet Impingement

See 1.1 and 3.4.

7. Cavity Response Phenomena

7.1 Ingard U., and Dean L.W., "Excitation of Acoustic Resonators by Flow", 2nd Symposium on Naval Hydrodynamics, pp 137-151, Aug 1958.

7.2 Krishnamurty K., "Acoustic Radiation From Two-Dimensional Rectangular Cutouts in Aerodynamic Surfaces", NACA TN 3487, August 1955.

7.3 Plumblee H.E., Gibson J.S., and Lassiter L.W., "A Theoretical and Experimental Investigation of the Acoustic Response of Cavities in an Aerodynamic Flow", WADD-TR-61-75, March 1962.

7.4 Roshko A., "Some Measurements of the Flow in a Rectangular Cut-Out", NACA TN 3488, Aug 1955.

7.5 Rossiter J.F., "Wind Tunnel Experiments on the Flow over Rectangular Cavities at Subsonic and Transonic Speeds", Royal Aircraft Establishment Technical Report 64037, October 1964.

8. Base Pressure Fluctuations

8.1 Eldred K. McK., "Base Pressure Fluctuations", JASA 33, 1 pp 59-63, January 1961.

See also 4.14.

TABLE I

TYPICAL CHARACTERISTICS OF VARIOUS FLUCTUATING PRESSURE SOURCES

Source	Ratio Root Mean Square Pressure to Total Head p_{rms}/q	Equivalent Sound Pressure for Typical Large Launch Vehicle Trajectory in dB(re 0. 00002 N/m^2
Attached Boundary Layer Turbulence	0.005 - 0.01	139 - 145
Base Pressure Fluctuations	0.01 - 0.02	145 - 151
Protuberance Flows	0.01 - 0.1 (locally)	145 - 165
Cavity Response	0.02 - 0.35	154 - 175
Separated Turbulent Flow	0.02 - 0.1	151 - 165
Oscillating Shock	0.05 - 0.1 (Supersonic) 0.05 - 0.25 (Transonic)	159 - 165 157 - 171

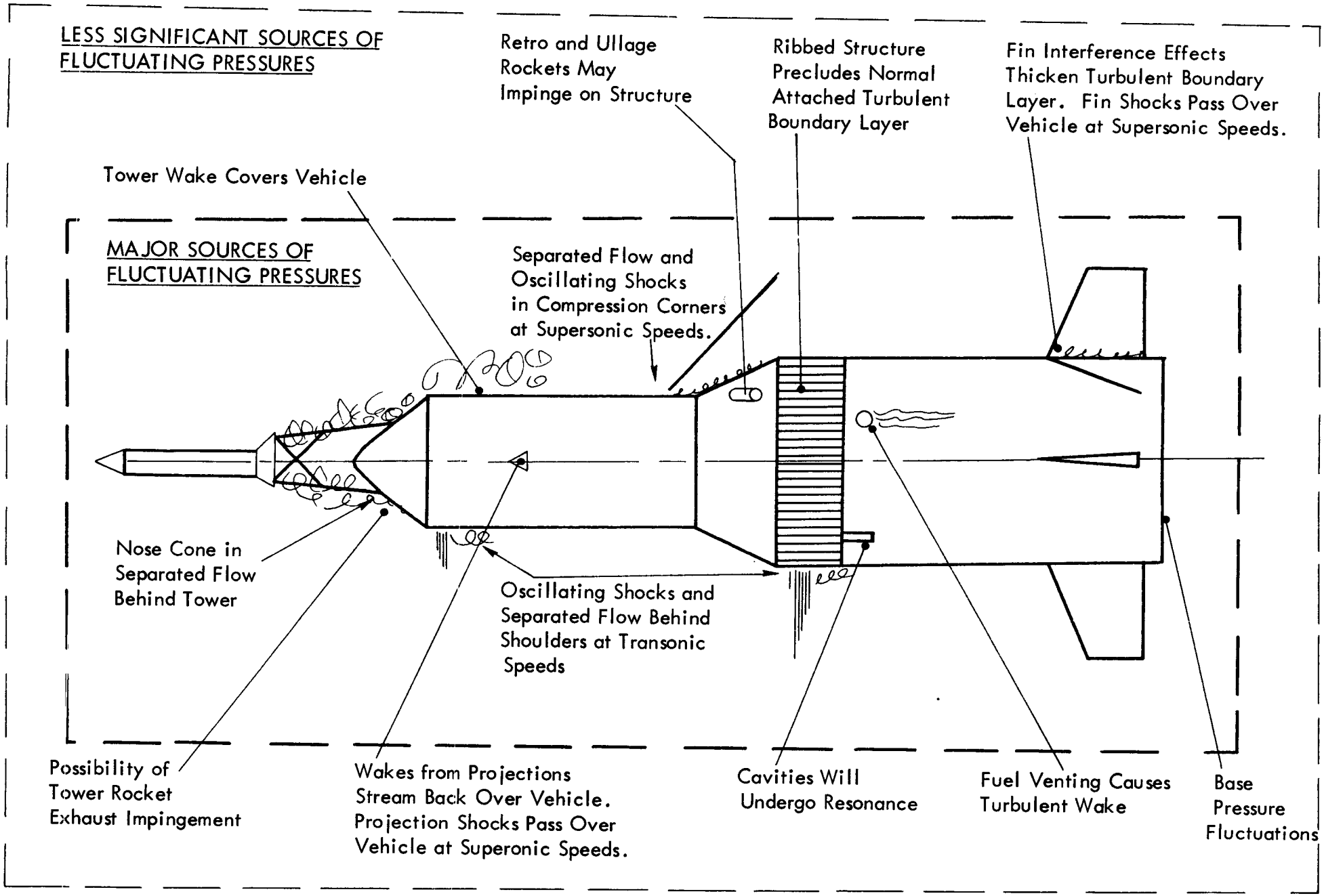

Figure 1. Typical Sources of Fluctuating Pressures on a Hypothetical Space Vehicle.

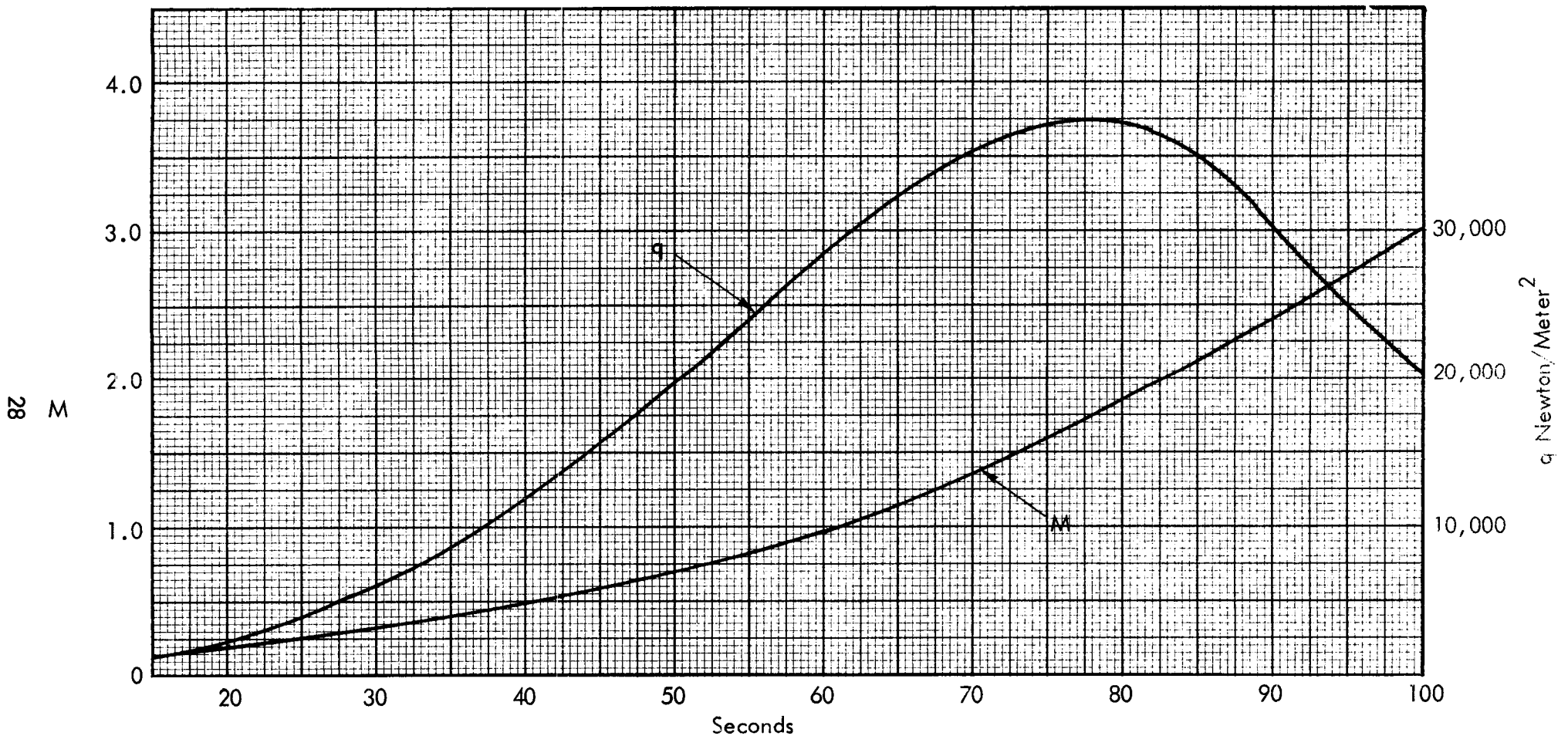

Figure 2. Mach Number and Total Head History for a Typical Large Launch Vehicle.

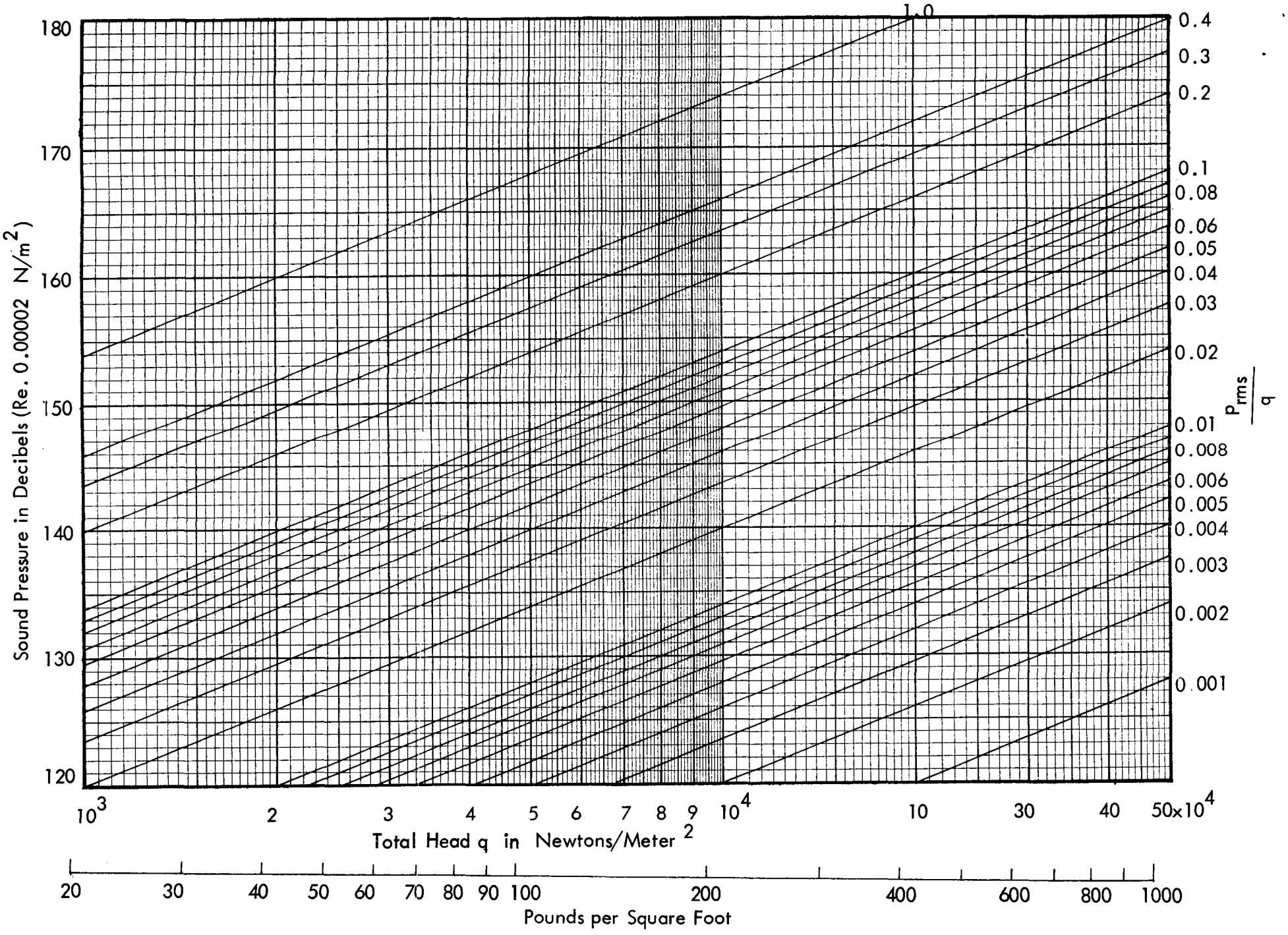

Figure 3. Conversion Chart for p_{rms}/q to dB.

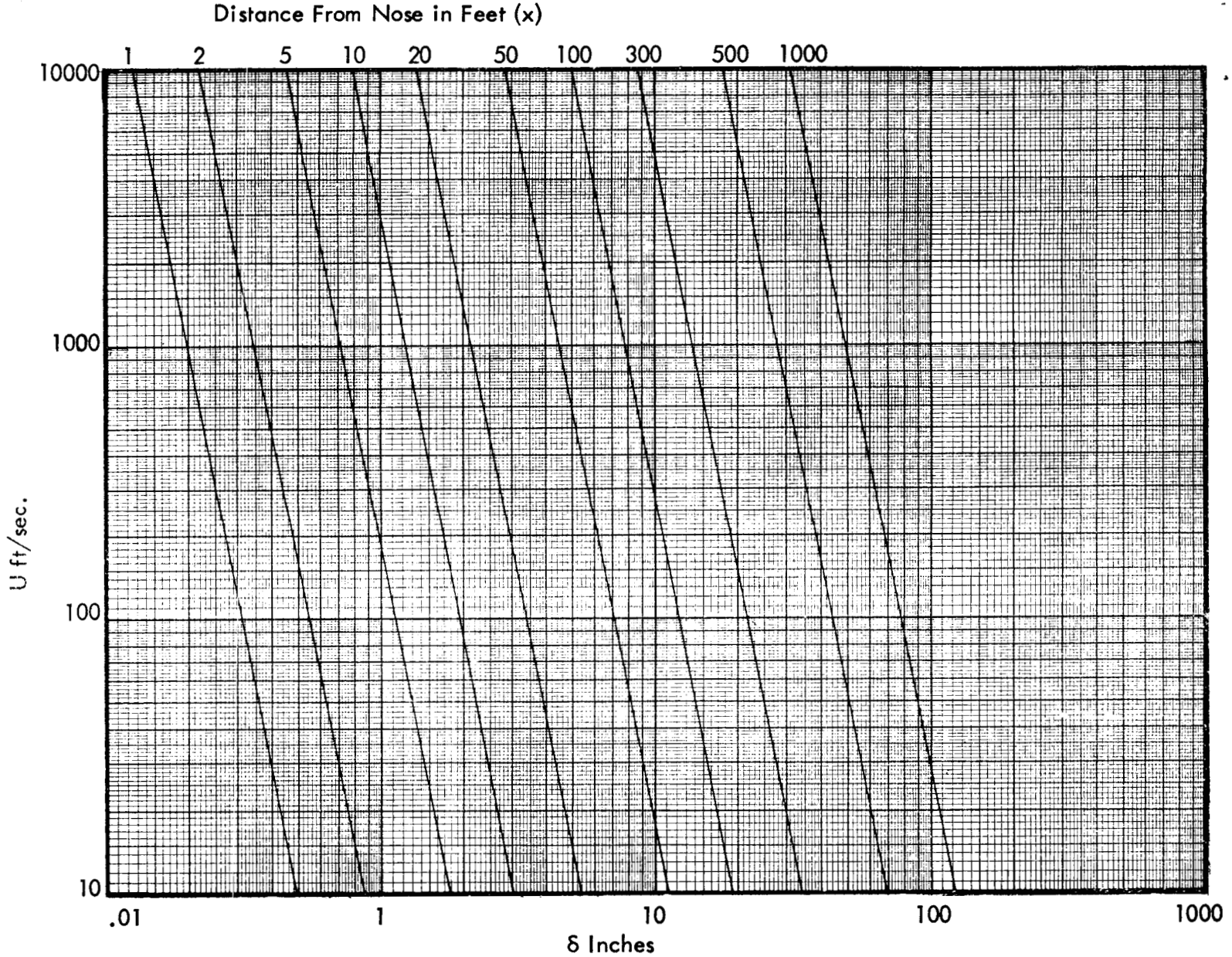

Figure 4. Boundary Layer Thickness From $\frac{\delta}{x} = \frac{0.376}{Re_x^{0.2}}$

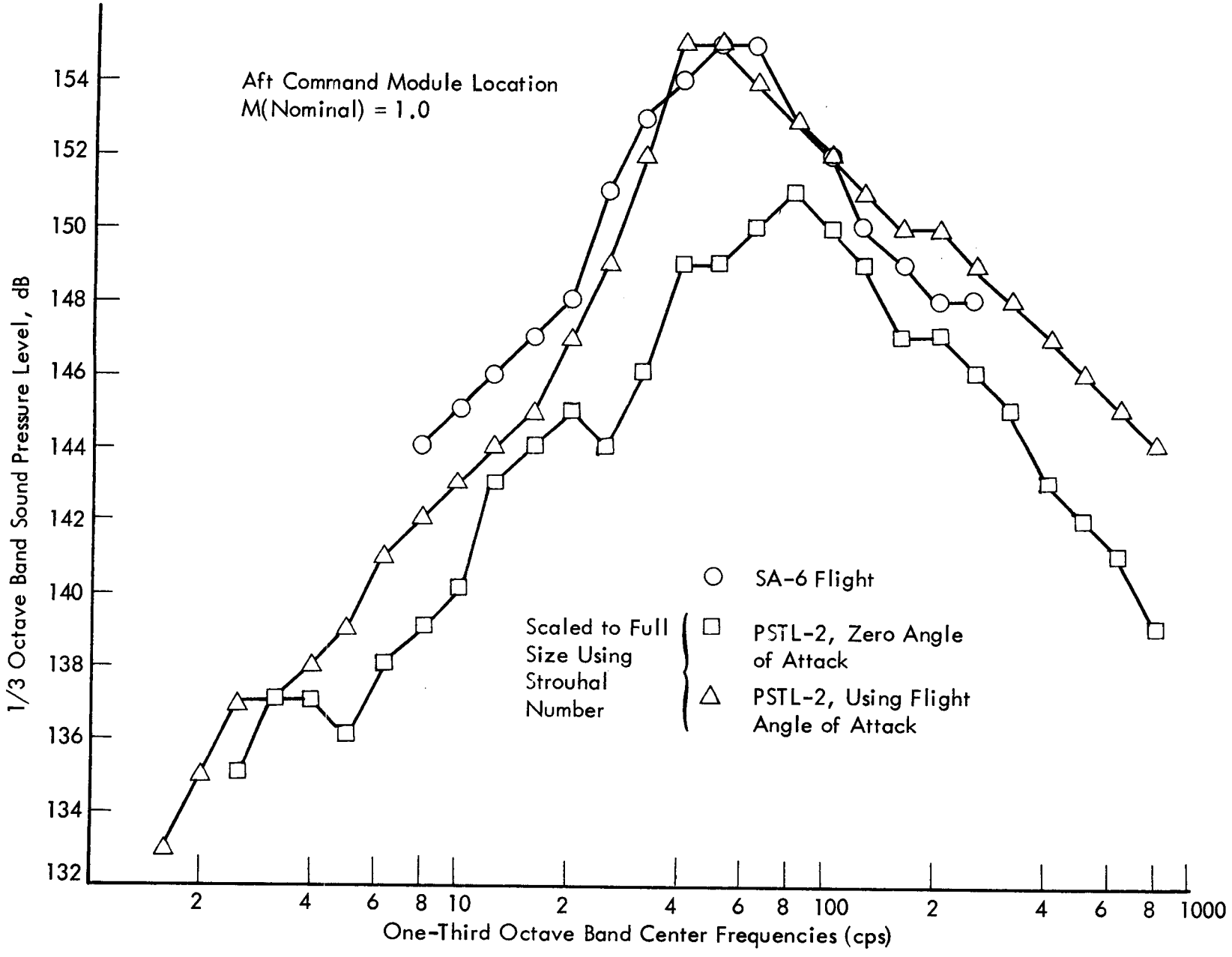

Figure 5. Comparison of 1/3 - Octave Band Spectra of Noise Measured on SA-6 Flight and in PSTL-2 Wind Tunnel Model Test. (From Reference 2.9).

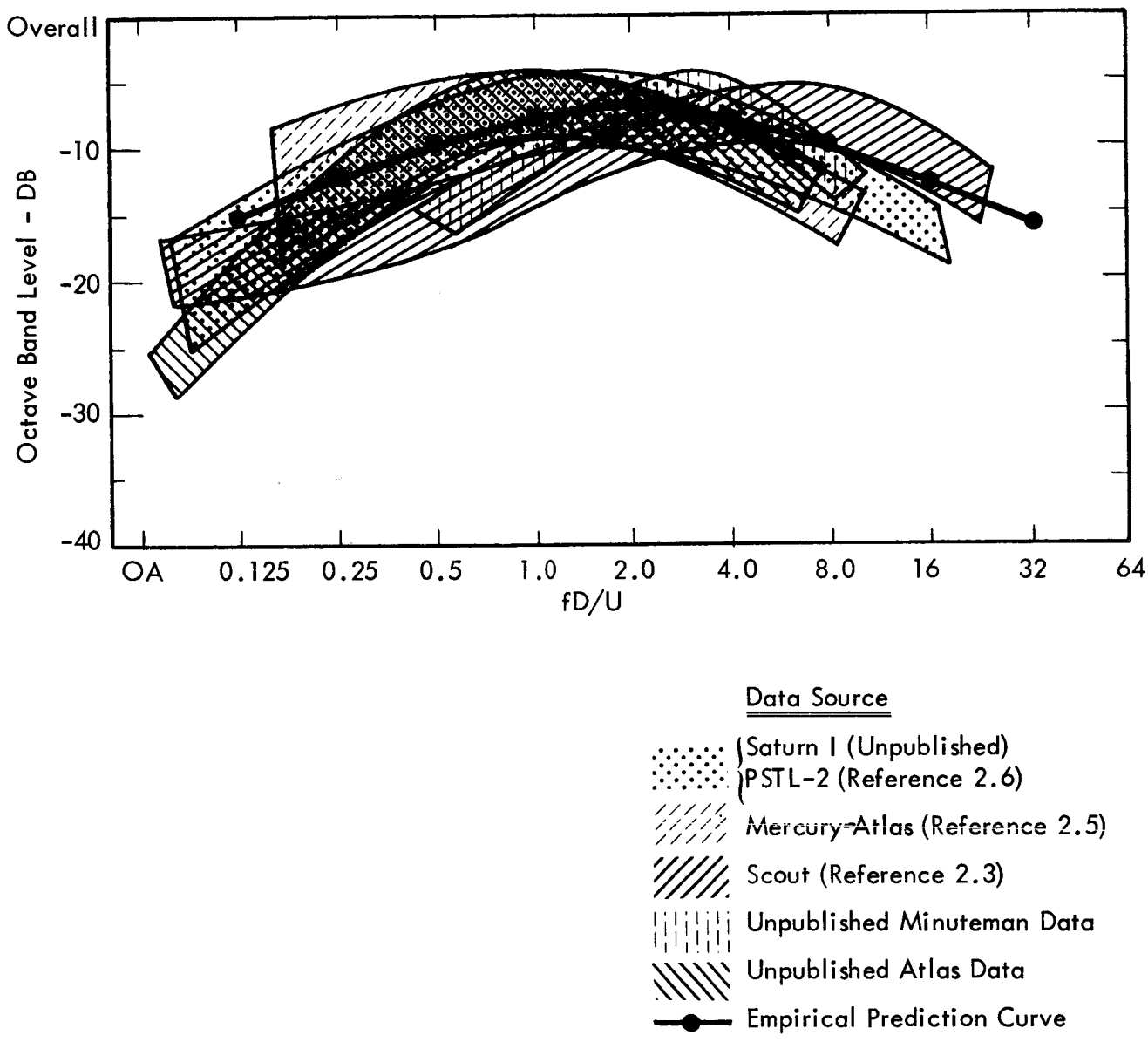

Figure 6. Non-Dimensionalized Fluctuating Pressure Spectra For a Number of Launch Vehicles.

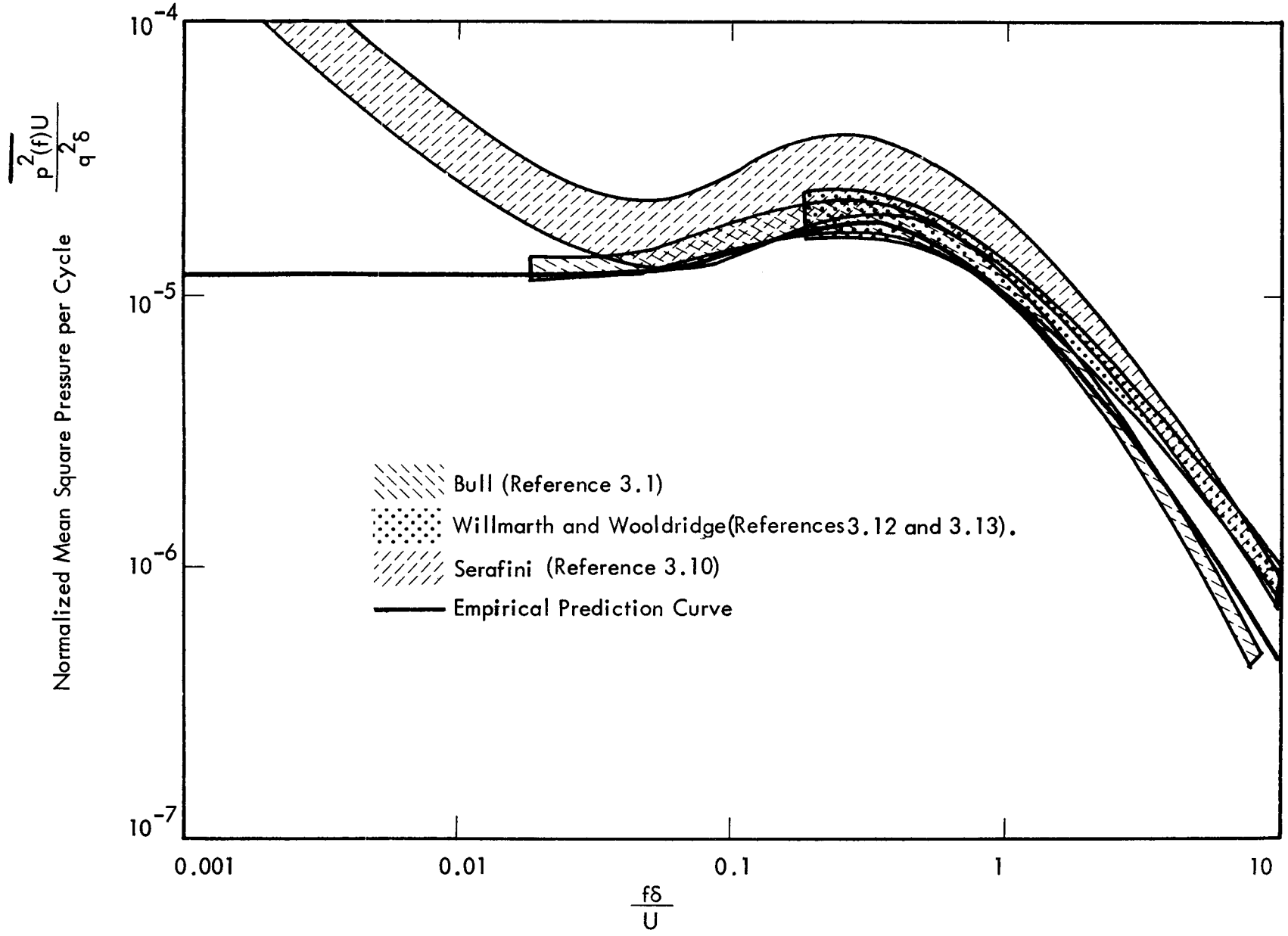

Figure 7. Fluctuating Pressure Spectra in an Attached Subsonic Boundary Layer.

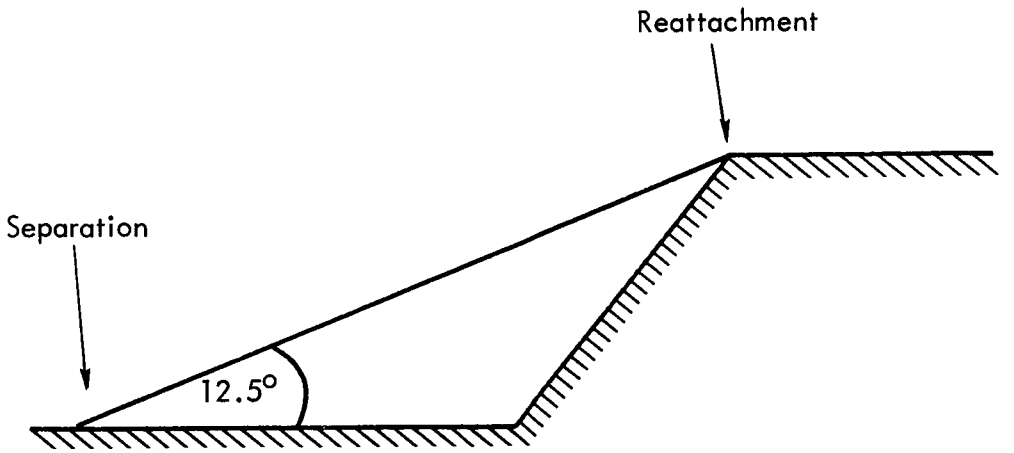

Figure 8a: Model Separation and Reattachment.

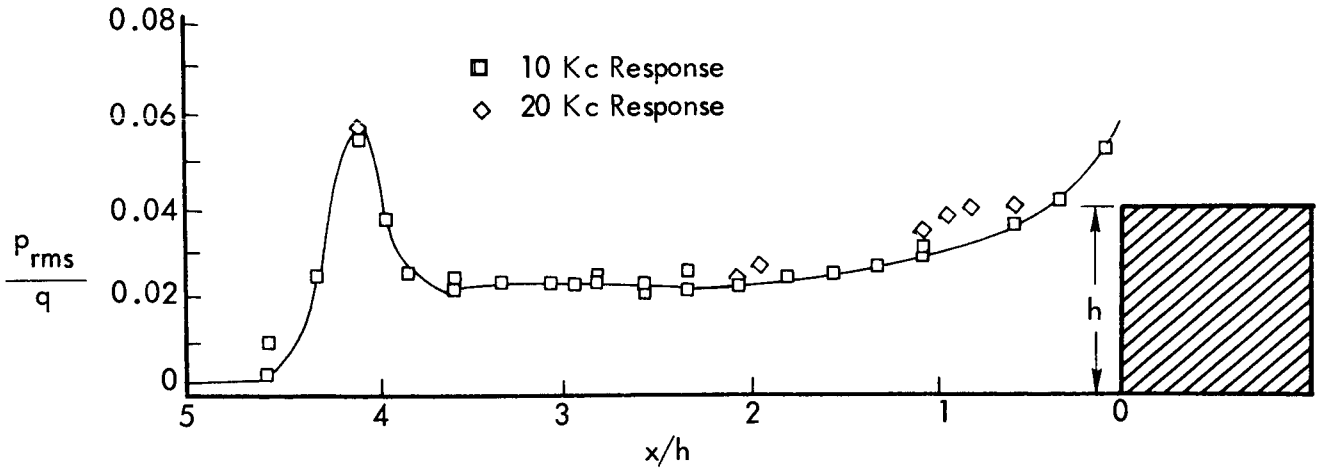

Figure 8b. Typical Fluctuating Pressure Distribution. (From Reference 4.14).

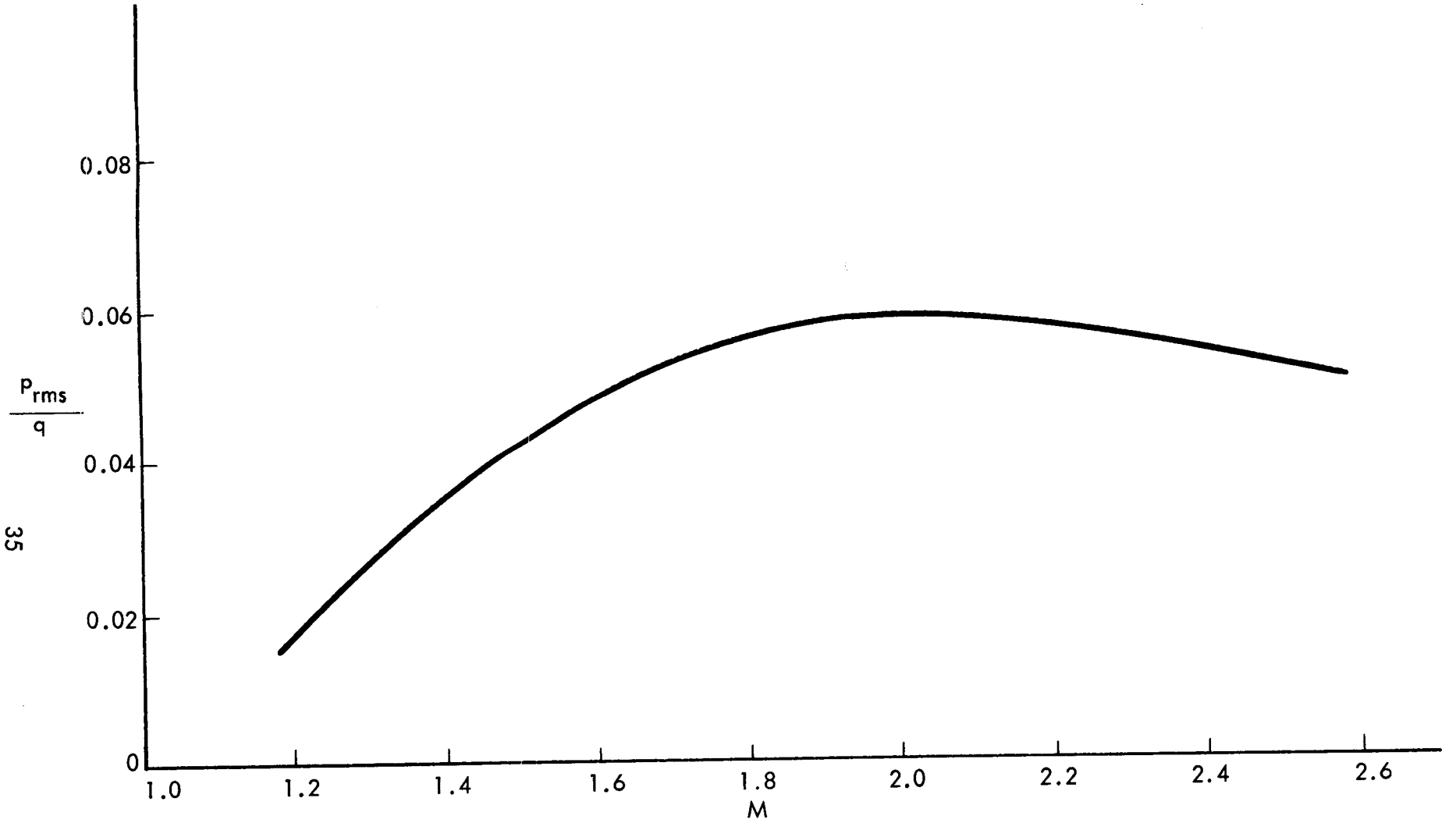

Figure 9. Peak Pressure Fluctuations vs Mach Number from Ames Data. (From Reference 4.14).

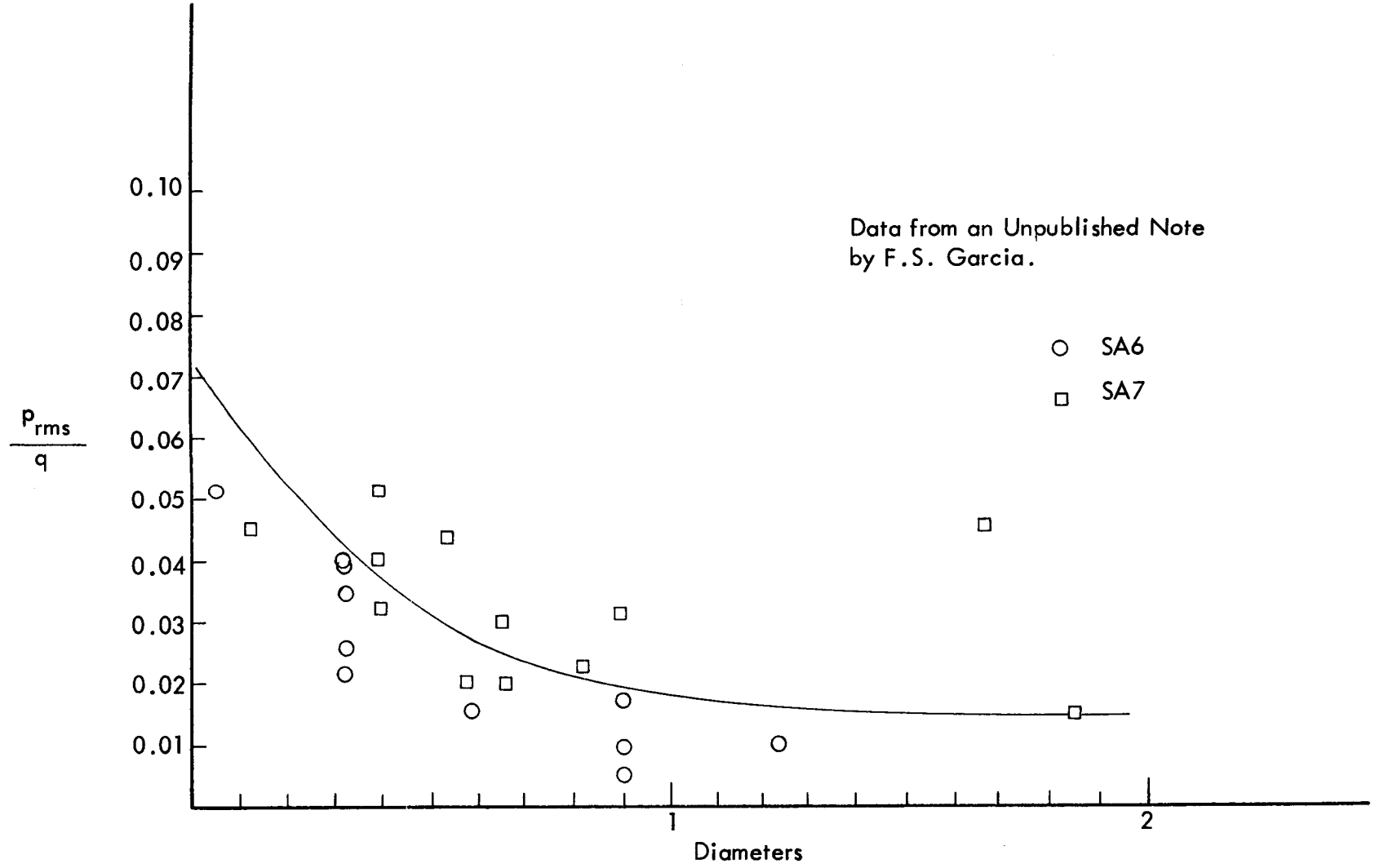

Figure 10. Fluctuating Pressures Measured Behind the First Shoulder During Flight.

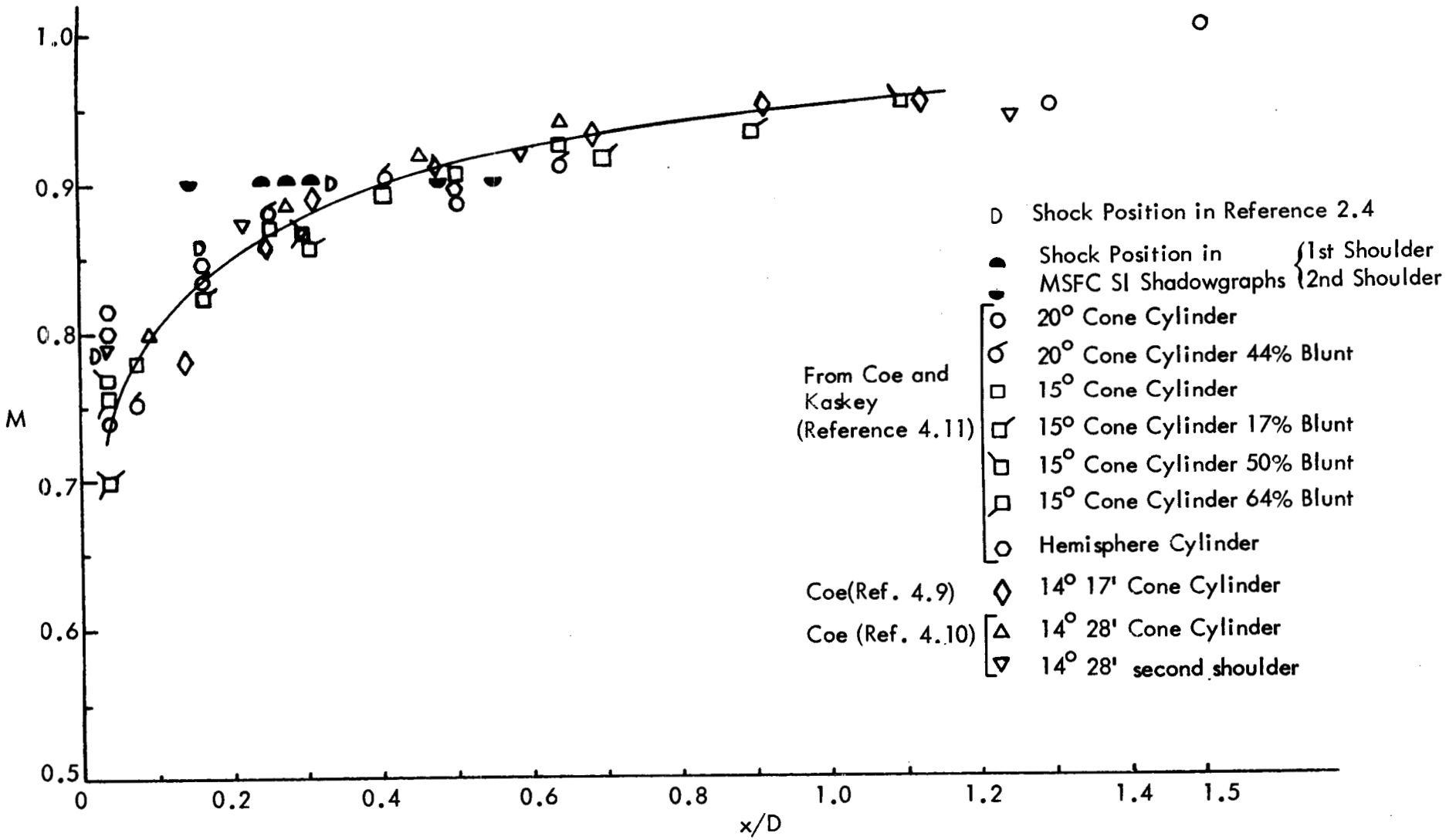

Figure 11. Position of Maximum $\frac{p_{rms}}{q}$ Behind Shoulder for Transonic Buffet.

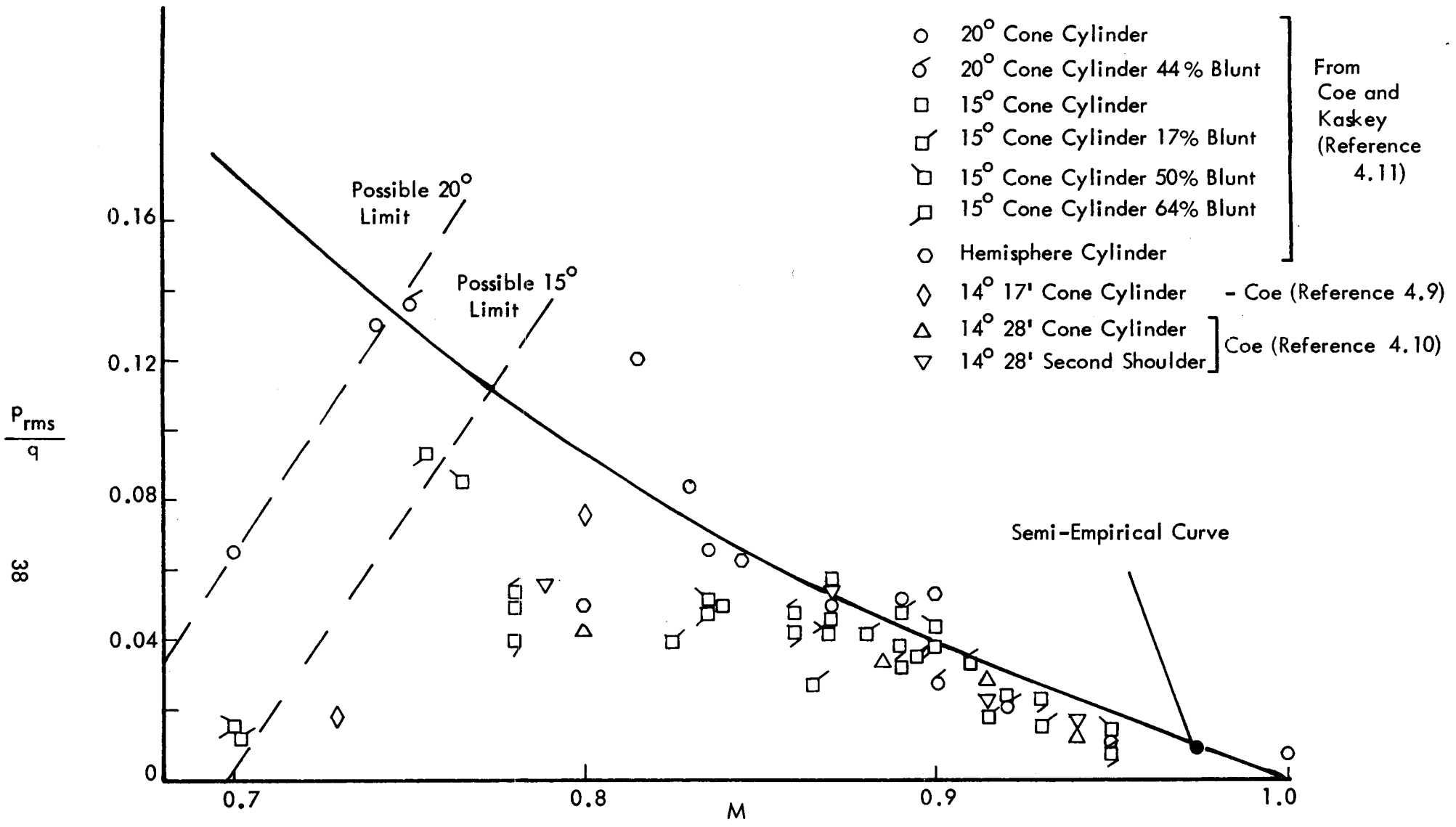

Figure 18. Fluctuating Pressure Under Transonic Oscillating Shock vs Mach Number

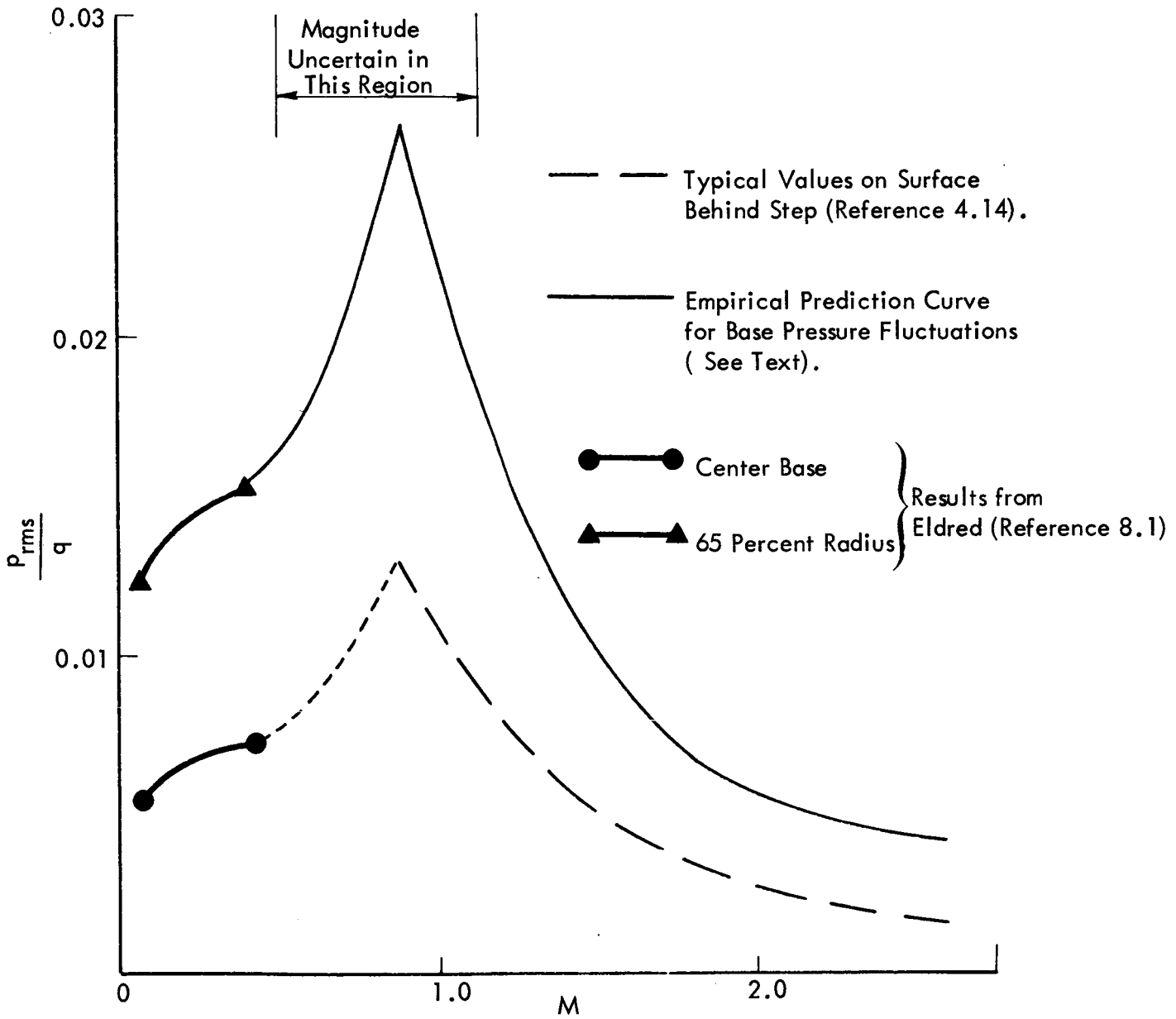

Figure 13. Estimated Magnitude of Base Pressure Fluctuations.

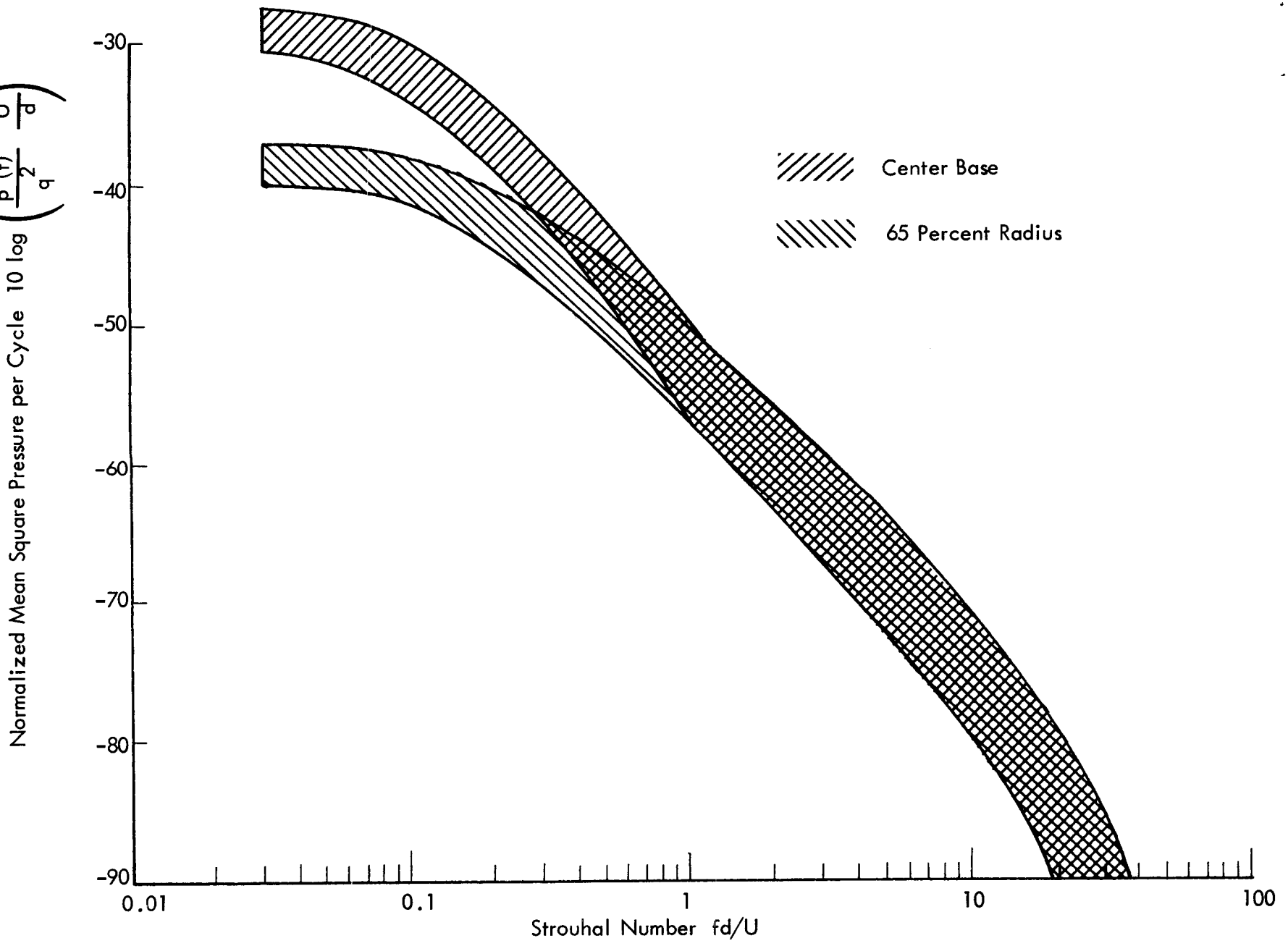

Figure 14. Fluctuating Base Pressure Spectrum Given by Eldred (Reference 8.1)